AGU PUBLICATIONS

Paleoceanography

RESEARCH ARTICLE
10.1002/2014PA002698

Key Points:
- Agulhas Bank slope hydrography is estimated from geochemical reconstructions
- Agulhas hydrographic indicators vary with Northern Hemisphere cool periods

Supporting Information:
- Readme
- Figure S1
- Figure S2
- Figure S3
- Figure S4
- Figure S5
- Figure S6

Correspondence to:
K. A. Dyez,
kdyez@ldeo.columbia.edu

Citation:
Dyez, K. A., R. Zahn, and I. R. Hall (2014), Multicentennial Agulhas leakage variability and links to North Atlantic climate during the past 80,000 years, *Paleoceanography*, *29*, 1238–1248, doi:10.1002/2014PA002698.

Received 10 JUL 2014
Accepted 26 NOV 2014
Accepted article online 29 NOV 2014
Published online 18 DEC 2014

Multicentennial Agulhas leakage variability and links to North Atlantic climate during the past 80,000 years

Kelsey A. Dyez[1,2], Rainer Zahn[1,3], and Ian R. Hall[4]

[1]Institut de Ciència i Tecnologia Ambientals, Universitat Autònoma de Barcelona, Bellaterra, Spain, [2]Now at Lamont-Doherty Earth Observatory, Columbia University, Palisades, New York, USA, [3]Institució Catalana de Recerca i Estudis Avançats, Departament de Fisica, Universitat Autònoma de Barcelona, Bellaterra, Spain, [4]School of Earth and Ocean Sciences, Cardiff University, Cardiff, UK

Abstract New high-resolution sea surface temperature (SST) and sea surface salinity (SSS) estimates are presented from the Agulhas Bank slope in the Atlantic sector of the Agulhas Corridor using planktic foraminiferal (*Globigerinoides ruber*) $\delta^{18}O$ and Mg/Ca-derived SST. By focusing on the last 80,000 years, this is the first fine-scale Agulhas leakage record that overlaps in time with much of the Greenland ice core record of abrupt climate changes in the North Atlantic region. The multicentennial profiles indicate instances of warm SST and/or increased SSS coincident with Northern Hemisphere cool periods, followed by Northern Hemisphere warming. These periods of enhanced SST and SSS in the Agulhas Corridor occur at the last glacial termination (T1) and during North Atlantic cold episodes associated with Heinrich (H) meltwater events. To a first-order approximation, the timing of maximal salinity events in relation to periods of North Atlantic freshwater perturbation is consistent with the concept suggested by climate models that enhanced Agulhas leakage provides for buoyancy compensation and can potentially trigger increased convective activity in the North Atlantic, thereby restoring Atlantic overturning circulation after relatively weak states.

1. Introduction

Climate variability in the Northern Hemisphere on orbital to suborbital time scales is widely linked to changes in the Atlantic meridional overturning circulation (AMOC) [*Clark et al.*, 2002; *McManus et al.*, 2004]. While the overall circulation is largely driven by the balance of energy input from the surface wind field and tidal mixing in the ocean's interior [*Ganachaud and Wunsch*, 2000; *Wunsch and Ferrari*, 2004], buoyancy variations contribute to the vertical mixing of seawater and can drive transient changes of the AMOC [*Kuhlbrodt et al.*, 2007]. In turn, surface ocean circulation can drive rapid changes in Northern Hemisphere ice sheets, atmospheric convection, and continental temperatures [e.g., *Boyle and Keigwin*, 1987; *Keigwin et al.*, 1991]. Numerical modeling suggests that the buoyancy forcing needed to stimulate transient shifts of AMOC strength depend in part upon the transport of high-salinity surface water from the Indian Ocean to the South Atlantic by way of Agulhas saltwater leakage [*Weijer et al.*, 2001; *Biastoch et al.*, 2008a, 2008b; *Beal et al.*, 2011; *Rühs et al.*, 2013].

The hydrodynamics of the modern Agulhas Current and its leakage into the South Atlantic reflect the interplay of the westerly wind field and the position of the Agulhas retroflection; ultimately, these factors allow for a portion of Agulhas Current surface waters to flow into the South Atlantic via rings, filaments, or patches [*Lutjeharms*, 1996; *Boebel et al.*, 2003; *Loveday et al.*, 2014]. Modeling results suggest that as westerly winds shift equatorward, Agulhas leakage is enhanced and potentially contributes to AMOC stability [*Durgadoo et al.*, 2013]. Changes in atmospheric circulation associated with the recent warming over the past three decades may also have allowed for enhanced Agulhas leakage, potentially offsetting the effect of concurrent North Atlantic freshening on the AMOC [*Biastoch et al.*, 2009; *Rouault et al.*, 2009]. Yet uncertainties remain in fully understanding the dynamics of Agulhas leakage over the range of climate-relevant time scales [*Beal et al.*, 2011] and its significance for deepwater formation in the North Atlantic [*de Ruitjer et al.*, 1999; *Marino et al.*, 2013]. Quantitative paleohydrographic data from this region is therefore critical to estimate past Agulhas salt-leakage variability and to assess its link with North Atlantic climate.

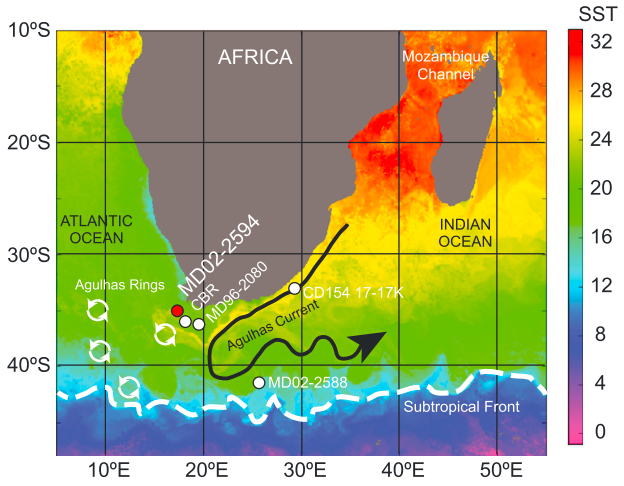

Figure 1. Schematic of Agulhas system with location of Agulhas slope core MD02-2594. The background colors are high-resolution satellite-observed SST during austral summer (1 January 2013; G1SST) [*Jet Propulsion Laboratory*, 2014]. The site of the Cape Basin Record [*Peeters et al.*, 2004] and MD96-2080 [*Martínez-Méndez et al.*, 2010] are shown for reference.

Paleoceanographic investigations into Agulhas Current variability largely aim to constrain Agulhas saltwater leakage in terms of the timing and magnitude of past leakage events in relation to Southern Hemisphere and North Atlantic climate variability [*Rau et al.*, 2002; *Peeters et al.*, 2004; *Rau et al.*, 2006; *Martínez-Méndez et al.*, 2010; *Caley et al.*, 2011, 2012; *Marino et al.*, 2013; *Simon et al.*, 2013; *Caley et al.*, 2014]. To this end, multicentennial to millennial time scale records of hydrographic variability in the Agulhas leakage Corridor have recently been published for the previous two glacial-interglacial climate cycles of marine oxygen isotope stage (MIS) 8-MIS 5 (265 ka–77 ka) [*Marino et al.*, 2013] and upstream in the Agulhas Current for the last glacial cycle (100 ka to present) [*Simon et al.*, 2013]. These studies suggest that Agulhas leakage varied at orbital and millennial scales and that abrupt leakage events often coincided with North Atlantic cold events that are depicted in marine records from the western Iberian Margin [*Marino et al.*, 2013]. In this study we present surface ocean hydrographic reconstructions of the past 80 kyr to further assess the heat and salt contents of Agulhas leakage and the timing of leakage events in the context of abrupt North Atlantic climate variability and the Atlantic's bipolar seesaw [*Stocker and Johnsen*, 2003]. By focusing on the last 80 kyr, this is the first fine-scale Agulhas surface leakage record that overlaps in time with the Greenland ice core record of abrupt climate changes in the North Atlantic region [*North Greenland Ice Core Project* (*NGRIP*) *Members*, 2004].

2. Methods

We generated quantitative reconstructions of surface-ocean hydrographic variability from marine sediment core MD02-2594 (34°42.6'S, 17°20.3'E; water depth of 2440 m) that was retrieved during the R/V *Marion Dufresne* cruise MD128 "South West Africa Campaign" [*Giraudeau et al.*, 2003]. The core location on the Agulhas Bank slope is directly influenced by deep-reaching Agulhas rings, which constitute the prime mechanism of Agulhas saltwater leakage into the Atlantic [*Lutjeharms*, 1996] (Figure 1). Our combined Mg/Ca-based sea surface temperature (SST) and oxygen isotope ($\delta^{18}O$) records were derived from the analysis of the tropical/subtropical surface-dwelling planktic foraminifera *Globigerinoides ruber* (white, in a strict sense) and span the past 80 kyr. Core MD02-2594 is a component of the "Agulhas Bank Splice" that was previously published by *Martínez-Méndez et al.* [2010], who presented similar $\delta^{18}O$ and Mg/Ca-based SST records derived from the planktic foraminifera *Globigerina bulloides*. However, this subsurface (50–100 m water depth) dwelling species has an affinity to nutrient availability, and its life habitat seems largely unaffected by ambient temperature, being reported from almost every SST range in the world oceans [*Bé and Hutson*, 1977; *Hemleben et al.*, 1989; *Sautter and Thunell*, 1989]. Therefore, it is not strictly representative of subtropical waters carried by the Agulhas Current. Indeed, results from *G. bulloides* were not fully consistent with complementary data profiles (e.g., alkenone-based SST estimates [*Peeters et al.*, 2004]) from neighboring cores. In this study we use *G. ruber* as a species more intimately adapted to the subtropical surface waters of the Agulhas Current, and note that it is also included as a faunal component in the so-called "Agulhas Leakage Fauna" [*Peeters et al.*, 2004].

Samples were analyzed every ~2 cm from 0 to 7.5 mcd, thereby enhancing the temporal resolution of preexisting records from this core [*Martínez-Méndez et al.*, 2010] by an average of 85 years, from average time steps of 385 years to ~300 years. For each sample, 55–70 *G. ruber* tests were picked from the 250–355 μm size fraction, crushed, homogenized, and split into aliquots: ~400 μg for minor and trace element analysis,

~30 μg for stable isotope analysis, and ~400 μg reserved for replicate analyses as needed. Samples for minor and trace element analysis were cleaned following established protocols, including oxidation and reduction steps [*Boyle and Keigwin*, 1985; *Mashiotta et al*., 1999]. Elemental ratios of planktic foraminifera were measured via an Agilent 8800 Quadropole inductively coupled plasma–mass spectrometry at the Universitat Autònoma de Barcelona (UAB); 1σ standard deviation for repeat Mg/Ca measurements of internal foraminifera reference standards was 0.12 mmol/mol. To monitor sample cleaning, Mn, Al, and Fe concentrations were measured in each sample and reference standards [*Boyle*, 1983; *Barker*, 2003; *Pena et al*., 2005]; no samples were removed via this screening. The depth of the core is well above the lysocline; based on shell weights, *Martínez-Méndez et al*. [2010] found no evidence for partial dissolution. We calculated SST based on calibration curves for surface water shell calcite using a species-specific calibration for *G. ruber*: SST = ln [Mg/Ca/0.449]/0.09 [*Anand et al*., 2003]. The reconstructed SST carries a propagated 1σ error, including analytical and calibration errors, of ±1.3°C.

The original age model for core MD02-2594 (here referred to as MM2010) was developed by *Martínez-Méndez et al*. [2010] based on 11 planktonic foraminifera radiocarbon dates for the period of 0–45 kyr and graphical correlation of benthic $\delta^{18}O$ with the high-resolution record of core MD97-2120 from the southwest Pacific for the period of 45–80 kyr (45°32′S, 174°57′E) [*Pahnke et al*., 2003; *Pahnke and Zahn*, 2005]. This age model had been synchronized with the benthic $\delta^{18}O$ records of Iberian Margin cores MD01-2443 and MD01-2444 [*Shackleton et al*., 2000] and the North Greenland Ice Core Project (NGRIP) Greenland ice core chronology [*Pahnke et al*., 2003; *Pahnke and Zahn*, 2005] (Figure S1 in the supporting information). Here it is reexamined. We first tested whether the European Project for Ice Coring in Antarctica (EPICA) Dome C (EDC3) age model produces measurable deviations from the MM2010 time scale. We did this by first tuning the MD97-2120 SST profile to EDC δD [*Jouzel et al*., 2007] on the EDC3 time scale and transferring these ages to the MD97-2120 benthic $\delta^{18}O$ record [*Pahnke et al*., 2003; *Pahnke and Zahn*, 2005]; the MD02-2594 benthic $\delta^{18}O$ record was then graphically tuned to the MD97-2120 benthic $\delta^{18}O$ record on its EDC3 age scale. For an additional comparison to the EDC3 time scale, we retuned the MD02-2594 benthic $\delta^{18}O$ profile to the benthic $\delta^{18}O$ profile of core MD02-2588 from the Agulhas Plateau to the south, which already has an EDC3 time scale [*Ziegler et al*., 2013] and transferred this age model to the MD02-2594 SST record. Beyond the section covered by ^{14}C-accelerator mass spectrometry (AMS) datums, age offsets between the MM2010 age model and revised EDC3 age models are insignificant (Figure S2 in the supporting information). We find that the original age model beyond the ^{14}C-AMS datums is compatible with the EPICA Dome C (EDC3) chronology [*Parrenin et al*., 2013] (Figure S2 in the supporting information). Thus, we maintained the original MM2010 chronology with the notable exception hence that the original ^{14}C dates are updated using the recent ^{14}C calibration curve of *Reimer et al*. [2013] and Calib 7.0 (http://calib.qub.ac.uk/calib/calmenu.cgi?datamenu), with an average of ΔR of 186 ± 66 from four nearby locations: http://calib.qub.ac.uk/marine/.

Stable isotope splits of *G. ruber* specimens were measured at UAB using a Thermo Scientific modern analog technique 253 mass spectrometer linked to a Kiel IV carbonate preparation device. External reproducibility of the analyses was monitored using international standards (International Atomic Energy Agency-CO-1 and NBS-19) with a 1σ $\delta^{18}O$ reproducibility of equal to or better than 0.08‰. Seawater $\delta^{18}O$ ($\delta^{18}O_{sw}$) was then estimated from paired $Mg/Ca_{G.\ ruber}$ and $\delta^{18}O_{G.\ ruber}$ measurements using the paleotemperature equation: $\delta^{18}O_{sw} = (SST - 16.5)/4.8 + \delta^{18}O_c + 0.27$ [*Bemis et al*., 1998]; given the average values for SST and $\delta^{18}O_c$, propagated uncertainty in $\delta^{18}O_{sw}$ is 0.28‰. An ice volume correction was made to obtain the local $\delta^{18}O_{sw}$ anomaly ($\Delta\delta^{18}O_{sw}$) by subtracting mean-ocean $\delta^{18}O_{sw}$ as estimated from sea level reconstructions. Age models of the sea level records are primarily based on ^{14}C dating for the past 40 ka and benthic $\delta^{18}O$ correlations to well-dated cores for the period of 40–80 kyr [*Arz et al*., 2007; *Grant et al*., 2012] and are compatible with the MD02-2594 age model, which is supported by tight correlation of inflection points into and out of MIS 4 and MIS 2 in both records (Figure S4 in the supporting information). Sea level data were converted to seawater $\delta^{18}O$ by applying an enrichment of 0.008‰/m of sea level lowering [*Schrag et al*., 2002].

3. Results

The $\delta^{18}O_{G.\ ruber}$ record follows a standard glacial-interglacial pattern, with a rapid increase in $\delta^{18}O$ at the MIS 4/5 transition (71 ka) by 0.6‰, a slight decrease during MIS 3, and a 1.2‰ decrease at the end of MIS 2 and

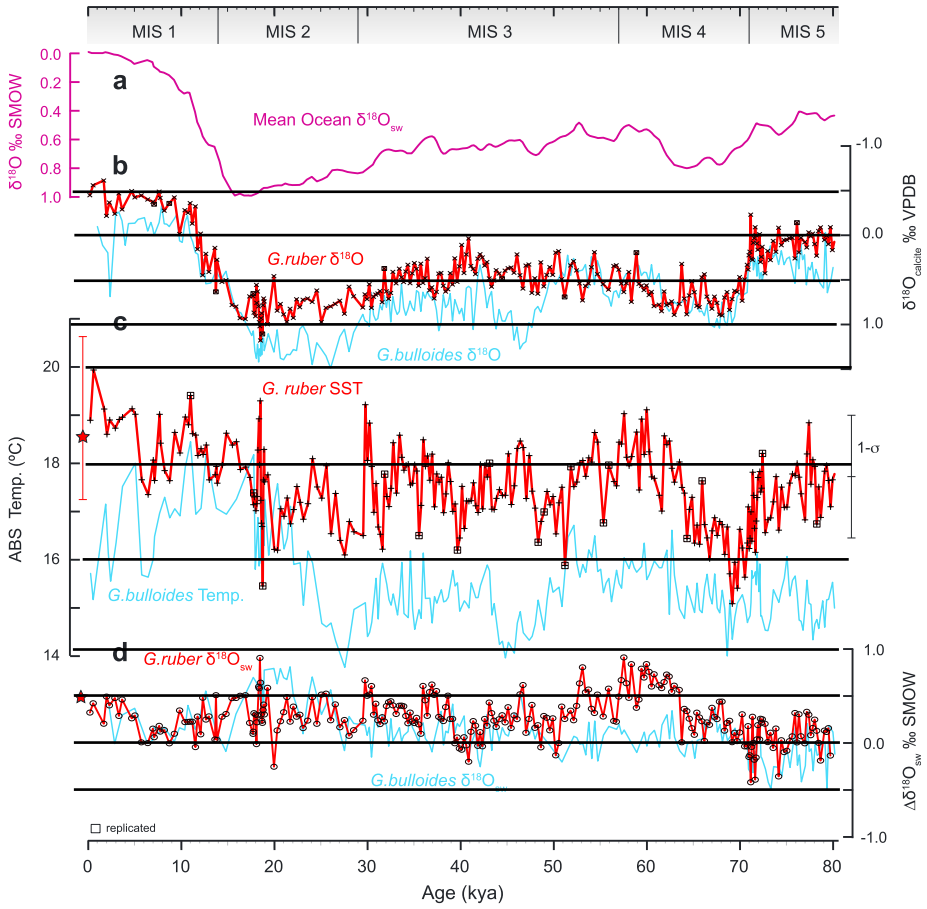

Figure 2. Global $\delta^{18}O_{sw}$ curve (violet) [*Arz et al.*, 2007; *Grant et al.*, 2012] compared with Agulhas Bank records of surface ocean hydrography from *G. ruber* (red line, *this study*) and from *G. bulloides* (blue) [*Martínez-Méndez et al.*, 2010]. (a) Mean ocean $\delta^{18}O_{sw}$, (b) $\delta^{18}O$ values of test calcite (inverse scale), (c) temperature based on Mg/Ca values (star and bar are the modern annual SST and summer/winter extremes) [*Locarnini et al.*, 2013], and (d) local $\delta^{18}O_{sw}$ anomaly derived from values in Figures 2a–2c and corrected for global sea level effects, with star for the modern value [*LeGrande and Schmidt*, 2006].

during T1 (Figures 2a and 2b). Comparing the $\delta^{18}O_{G.\ ruber}$ record with the $\delta^{18}O_{G.\ bulloides}$ profile of *Martínez-Méndez et al.* [2010] shows that both time series overlap during the early phase of the last glacial, between 72–52 ka and at T1, while during the rest of the time span, covered $\delta^{18}O_{G.\ bulloides}$ is enriched by 0.2–0.3‰ relative to $\delta^{18}O_{G.\ ruber}$ (Figure 2b); the $\delta^{18}O$ offset is in line with what would be expected given the potentially cooler temperatures recorded by the deeper dwelling *G. bulloides*; small differences in the offset may be related to surface water stratification, which could be a reflection of turbulent surface wind mixing either upstream from the core location or near the core location itself. The average Mg/Ca-based temperature difference between the SST profiles (Figure 2c) predicts a $\delta^{18}O$ difference between *G. ruber* and *G. bulloides* of 0.22‰ [*Bemis et al.*, 1998]; the actual average difference between $\delta^{18}O_{G.\ ruber}$ and $\delta^{18}O_{G.\ bulloides}$ profiles is 0.23‰. The slight offset between the values is within the range of analytical error.

In contrast to the $\delta^{18}O_{G.\ ruber}$ record, glacial-interglacial $Mg/Ca_{G.\ ruber}$-based SST variation is only weakly expressed at MD02-2594 (Figure 2c); the full range of values reaches from maximum SST of ~20°C near the core top, i.e., the latest Holocene, to minimum SST of ~16°C during early MIS 4. Using the $\delta^{18}O_c$ record to define T1 shows very little SST change across this transition (Figure 2c), which is unexpected given larger changes at glacial terminations observed in the *G. ruber* Mg/Ca-SST record of nearby core MD96-2080 during glacial terminations T3 and T2 [*Marino et al.*, 2013]. One reason for such a pattern may be that the last glacial transition (T1) tends to be somewhat smaller in the Southern Hemisphere than the previous termination (T2) as also seen in the EDC and EPICA Dronning Maud Land (EDML) ice core records [*European Project for Ice Coring in Antarctica* (*EPICA*) *Community Members*, 2006; *Jouzel et al.*, 2007]. A transient episode of cold SST is

seen during T1 at ~18.5 ka, although the magnitude of this SST change is also close to the propagated error of the SST reconstruction. Comparison with the Mg/Ca-based temperature of *Martínez-Méndez et al*. [2010] shows that estimates of calcification temperature derived from *G. bulloides* are typically some 2°C colder than those derived from *G. ruber* Mg/Ca ratios (Figure 2c). This result confirms the contention that *G. ruber*, as a tropical/subtropical species, is more uniquely linked with the tropical/subtropical waters carried by the Agulhas Current, while *G. bulloides*, in addition to living in warm Agulhas waters, may also carry cold water signals from outside the immediate Agulhas surface ocean domain. For example, *G. bulloides* has a known affinity for colder nutrient-rich upwelling waters and may be advected from the subantarctic zone by cross-frontal Ekman transport [*Martínez-Méndez et al*., 2010; *Naik et al*., 2013]. Further, modern annual average SST for this core site is within the uncertainty of the reconstructed core-top calcification temperature derived from *G. ruber* Mg/Ca but not that derived from *G. bulloides* Mg/Ca. The final notable difference between the two SST profiles is seen with the earlier warming in the *G. bulloides* record at the end of the last glacial, around 27 ka, starting some 10 kyr prior to the onset of warming recorded in the *G. ruber* SST record.

The close relationship between surface $\delta^{18}O_{sw}$ and surface salinity variations has been shown globally by *LeGrande and Schmidt* [2006] and for the Indian Ocean by *Singh et al*. [2010]. At the Agulhas Bank slope, the range in $\delta^{18}O_{sw}$ (−0.3 to 1.1‰) derived from paired *G. ruber* $\delta^{18}O$ and $SST_{Mg/Ca}$ is similar in magnitude to that previously derived from *G. bulloides* [*Martínez-Méndez et al*., 2010] and from *G. ruber* during MIS 6 [*Marino et al*., 2013]. In general, past $\delta^{18}O_{sw}$ maximizes during H events (Figures 2 and 3).

4. Discussion

4.1. Agulhas Leakage Variability Over the Past 80,000 Years

The Agulhas Bank slope is located in the path of the Agulhas leakage [*Lutjeharms*, 1996]; thus, SST and $\delta^{18}O_{sw}$ anomalies at this location can be viewed as a reflection of the hydrography of warm and high-salinity waters sourced in the western Indian Ocean that are transported to the South Atlantic Ocean. Our results show that the hydrography of the Agulhas Bank experienced a series of millennial scale fluctuations during the last glacial period (Figure 2). Several SST and $\delta^{18}O_{sw}$ excursions overlapped in timing with North Atlantic H event 1 (H1), H2, H3, H4, H5, and H6 [*Hemming*, 2004], while the peak coincident with H3 is most prominent (Figure 3). A transient SST maximum of 19°C is centered on ~14 ka, coinciding with the Bølling–Allerød (B-A) in the North Atlantic region and mid-T1 warming in Antarctica (Figure 3). The $\delta^{18}O_{sw}$ anomalies at this site suggest that North Atlantic Heinrich events were coincident with transient periods of increased salinity at the Agulhas Bank slope, which is consistent with enhanced saltwater transport to the South Atlantic (Figure 3).

However, such SST and $\delta^{18}O_{sw}$ excursions may have resulted from increased heat and/or salt retention in the Southern Hemisphere via the bipolar seesaw response to reduced AMOC during North Atlantic H events [*Barker et al*., 2009]. In order to assess this potential influence, we used the Antarctic EPICA Dome C δD temperature as a first-order indication of Southern Hemisphere temperature variability [*EPICA Community Members*, 2006; *Jouzel et al*., 2007]. We smoothed the Antarctic temperature record using a 1000 year wide moving mean and removed the long-term glacial-interglacial trend by subtracting a 7500 year moving mean smooth of the same record (Figure S5 in the supporting information). The residual temperature profile represents the millennial scale component of Antarctic temperature variability. When this millennial Antarctic temperature signal is compared with and removed from the MD02-2594 SST profile, several warm SST excursions become muted or disappear (11 ka, 16 ka, and 46 ka), while others become even more pronounced (at ~13 ka, 18 ka, 49 ka, and 73 ka) (Figure S5 in the supporting information). The SST anomalies coincident with the YD, H1, H2, and H3 persist as prominent warm events after the Southern Hemisphere signal is removed, which renders them independent from temperature developments in the Southern Hemisphere and identifies them as robust features related to the Agulhas Current hydrography. In contrast, those SST excursions that are eliminated with this normalization procedure may likely have been connected to Southern Hemisphere wide millennial scale fluctuations in temperature. An alternate ice core chronology [*Veres et al*., 2013] does not overall change these results (Figure 5 in the supporting information). Smaller SST and $\delta^{18}O_{sw}$ anomalies also occur outside the time windows of H events, but the fact that many anomalies are associated with H events highlights the dynamical linking of the Agulhas leakage with North Atlantic climatology.

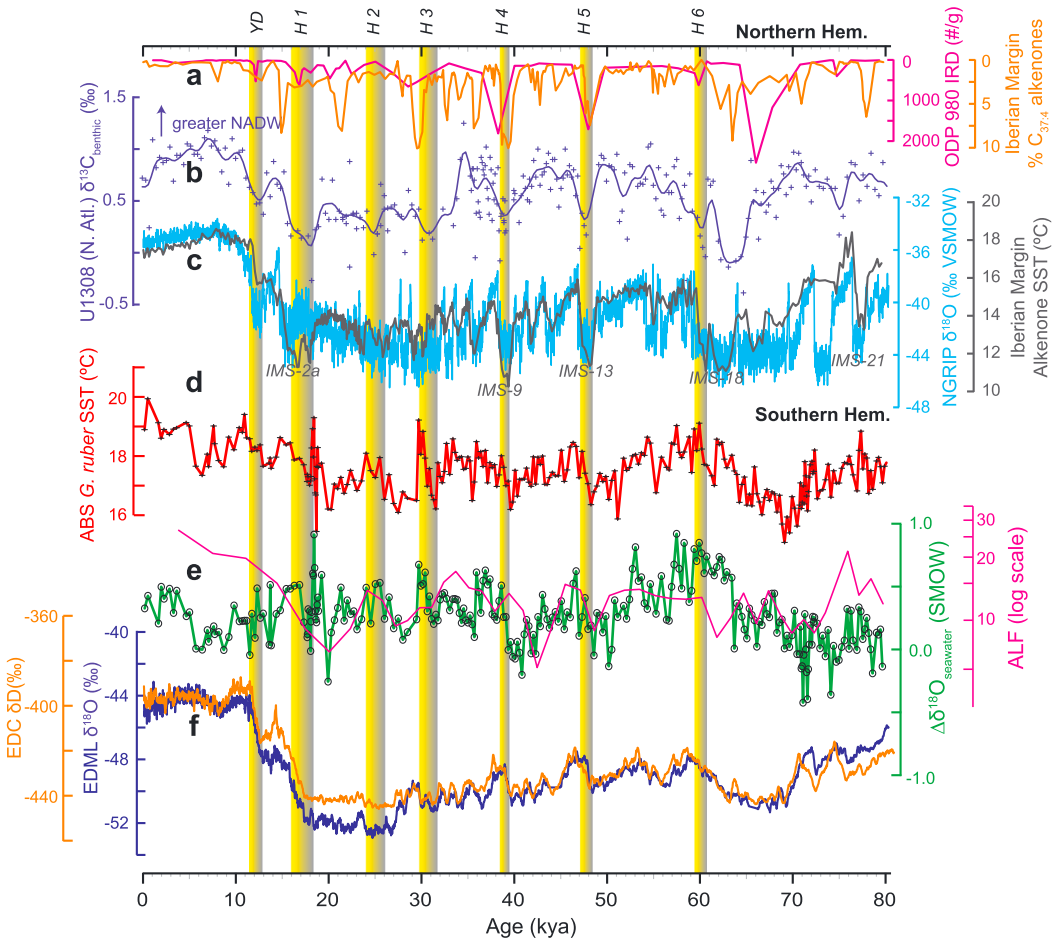

Figure 3. Northern Hemisphere links to the Agulhas Current and Southern Hemisphere, 80 ka to present. Northern Hemisphere: (a) IRD from Ocean Drilling Program (ODP) Site 980 (~55°N) (violet) [*McManus et al.*, 1999] and Iberian Margin (MD01-2343,4~38°N, orange) [*Martrat et al.*, 2007], (b) benthic carbon isotope record from Integrated Ocean Drilling Program Site U1308 (blue crosses with 1 kyr filter) [*Hodell et al.*, 2008], (c) NGRIP record of Greenland ice sheet $\delta^{18}O$ (light blue) [*NGRIP Members*, 2004], age model GICC05modelext [*Wolff et al.*, 2010], and Iberian Margin SST (black) [*Martrat et al.*, 2004] with selected Iberian Margin Stadials noted. Southern Hemisphere: (d) MD02-2594 *G. ruber*-based SST, (e) MD02-2594 *G. ruber*-based $\Delta\delta^{18}O_{sw}$ and Agulhas Leakage Fauna (pink) [*Peeters et al.*, 2004], (e) EDML $\delta^{18}O$ (blue) [*EPICA Community Members*, 2006], and EDC δD (orange) [*Jouzel et al.*, 2007].

4.2. Links to North Atlantic Climate

Previous estimates of Agulhas leakage hydrography also note the bipolar nature of millennial scale events in which Antarctic warming is contemporaneous with North Atlantic cooling [e.g., *Martínez-Méndez et al.*, 2010; *Marino et al.*, 2013]. This process has been described as a bipolar seesaw, one phase of which resulted in heat retention in the Southern Hemisphere [*Broecker and Denton*, 1989; *Stocker*, 1998; *Barker et al.*, 2009; *Skinner et al.*, 2010] and expansive formation of winter sea ice in the North Atlantic. This fostered the reorganization of atmospheric circulation, shifted the Intertropical Convergence Zone southward, and impacted the tropical Hadley cell and midlatitude southern westerlies [*Chiang*, 2009; *Lee et al.*, 2011]. The data pattern we observe between the North Atlantic and the Agulhas leakage area is conceptually consistent with such interhemispheric oceanic and atmospheric teleconnections.

To more firmly constrain whether such connections existed during the last glacial between Agulhas leakage oscillations and the modulation of AMOC strength and rapid Northern Hemisphere climate changes [*Weijer et al.*, 2002; *Knorr and Lohmann*, 2003; *Biastoch et al.*, 2008a; *Marino et al.*, 2013], we compare our record with the Greenland temperature profile, benthic $\delta^{13}C$ records from the North Atlantic, and Iberian Margin SST, which together reflect marine heat transport and North Atlantic Deep Water (NADW) formation driven by

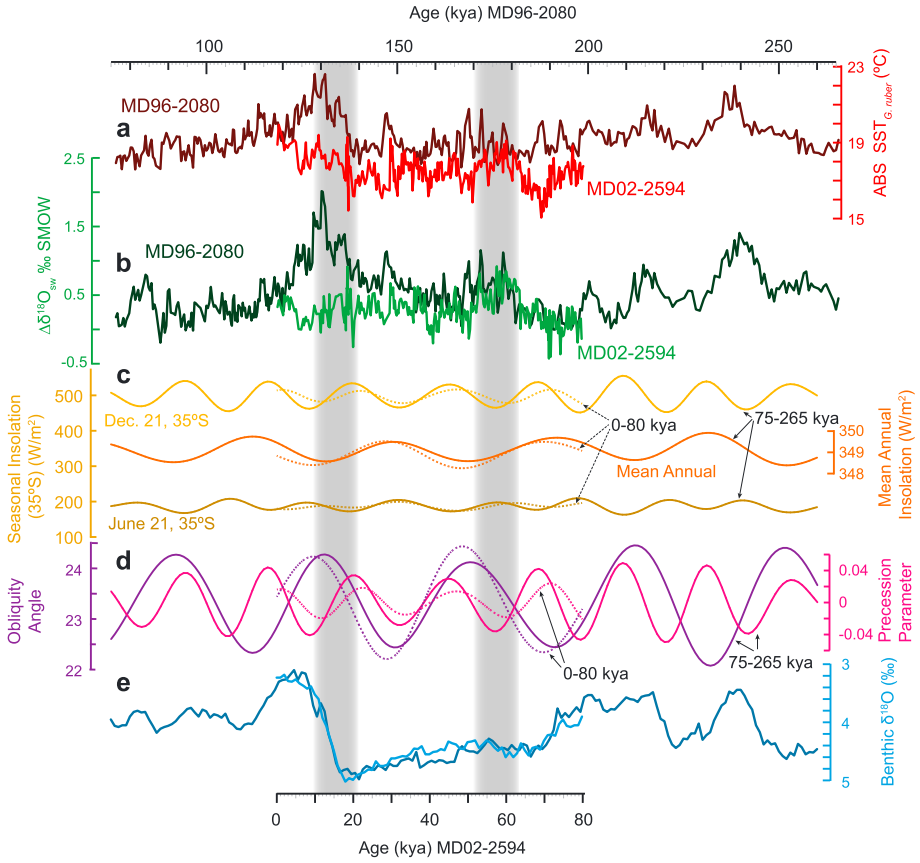

Figure 4. Comparison of (a) SST, (b) $\Delta\delta^{18}O_{sw}$, (c) calculated insolation and (d) orbital parameters [*Laskar et al.*, 2004], and (e) benthic calcite $\delta^{18}O$ [*Lisiecki and Raymo*, 2005] from 0–80 ka (MD02-2594) and 75–265 ka (MD96-2080) [*Marino et al.*, 2013]. The two time periods are primarily aligned via inflections in benthic $\delta^{18}O$. The vertical gray bars suggest two periods when Agulhas hydrography shows warmer SST and increased $\Delta\delta^{18}O_{sw}$.

AMOC strength (Figure 3). We observe that increased salt content of Agulhas leakage frequently coincides with cooler Greenland temperatures [*NGRIP Members*, 2004] such as during Heinrich events and the Younger Dryas when the North Atlantic experienced subpolar temperatures [*Martrat et al.*, 2007] and the AMOC weakened considerably as indicated by benthic $\delta^{13}C$ and uranium-series isotope profiles in the North Atlantic [*Hodell et al.*, 2008; *Lippold et al.*, 2009; *Waelbroeck et al.*, 2011]. Our age model does not allow us to determine when during the North Atlantic Heinrich events the leakage increased, if, for instance, the salt increase directly coincided with the cold events or if it was shifted toward the later stages of the Heinrich events as would be expected from numerical models which suggest a role for the leakage in bringing the AMOC out of freshwater-induced weakened states [*Weijer et al.*, 2001; *Biastoch et al.*, 2008a]. But coincidence, especially during Heinrich events, of increase in leakage during North Atlantic cold phases is consistent with the notion that increased salt leakage in the Southern Hemisphere contributed to the initiation of increased NADW formation after a period of freshwater perturbation in the Northern Hemisphere and slower overturning circulation (Figure 3). However, at other periods (21.5 ka or 2–4 ka), the connection is more ambiguous; at those times, the temperature and salinity oscillations may simply represent the natural variability of the Agulhas leakage independent from an interhemispheric forcing from the north.

4.3. Westerlies Support Agulhas Hydrography Changes

Recent climate model results suggest that Agulhas Current hydrography [*Simon et al.*, 2013] and salt leakage [*Durgadoo et al.*, 2013] respond sensitively to shifts in the intensity and latitudinal position of the southern westerlies. The response is transient and causes leakage to intensify when the westerly winds strengthen as a result of enhanced surface water recirculation within the southwest Indian subgyre and associated increased water transport to the Agulhas retroflection zone. Strengthened westerlies also

reinforce recirculation back into the Indian Ocean gyre as additional Agulhas water is retroflected into the southwest Indian Ocean subtropical gyre [*Durgadoo et al*., 2013; *Simon et al*., 2013]. The MD02-2594 $\Delta\delta^{18}O_{sw}$ profile is largely similar to that recently developed upstream in the Agulhas Current from core CD154 17–17 K (Figure S6 in the supporting information) [*Simon et al*., 2013], which suggests that hydrographic variability at both sites may indeed be connected through the southwest Indian subgyre circulation. However, small differences between the two records may reflect the circulation dynamics within the Indian-Atlantic Ocean gateway, for example, changes in the strength or position of the Agulhas retroflection, strength of the leakage, or changes in the salinity signature of the leakage and variable northward admixture of surface waters from the subantarctic zone to the south.

4.4. Does a Specific Orbital Configuration Support Increased Leakage?

Variations in the distribution of solar forcing have been invoked as one possible driver of multimillennial scale climate fluctuations [*Lisiecki et al*., 2008; *Toggweiler and Lea*, 2010; *Caley et al*., 2011, 2012]. To test whether Agulhas hydrography signals could be linked to a specific orbital configuration, we compared Agulhas leakage SST and sea surface salinity (SSS) anomalies during the last 80 kyr and those for 75–265 kyr from a neighboring core [*Marino et al*., 2013] with prevailing orbital and insolation parameters (Figure 4). The two SST and SSS sections were aligned using the benthic $\delta^{18}O$ series of each time span. Overall, SST and $\Delta\delta^{18}O_{sw}$ tend to increase alongside periods of increasing orbital obliquity as well as alongside diminishing annual insolation at 35°S latitude. This finding is consistent with previous work which suggested that increased Northern Hemisphere insolation (not shown) may be associated with a stronger AMOC at the 40 kyr periodicity [*Lisiecki et al*., 2008]. The orbital configuration of insolation may have affected surface hydrography at the core location by modulating the position of the subtropical front in relation to induced changes in westerly winds [*Peeters et al*., 2004]. When longer records of Agulhas leakage are considered, the dominant orbital signal is in the 100 kyr band [*Peeters et al*., 2004], although this may be due to irregular obliquity pacing [*Huybers and Wunsch*, 2005] or internal climate amplification [*Lisiecki*, 2010; *Caley et al*., 2011]. Although obliquity and precession variability are also present at lower spectral power in this record, both are coherent with incoming solar radiation, while variability in the 100 kyr band is not [*Peeters et al*., 2004]. While our record from MD02-2594 is not long enough to reveal power at eccentricity time scales, it does support the connection between increased salt leakage and Southern Hemisphere insolation minima at obliquity pacing.

5. Summary

Our results indicate that Agulhas salt leakage was a persistent feature of the Indian-Atlantic circulation during the past glacial period. SST and $\delta^{18}O_{sw}$ were reconstructed from Mg/Ca and $\delta^{18}O$ of *G. ruber*, a species that is more strictly representative of the subtropical waters transported in the Agulhas Current than *G. bulloides* which has been used previously for similar reconstructions [*Martínez-Méndez et al*., 2010]. The timing of several Agulhas salt maxima overlapped with North Atlantic Heinrich events and hence conceptually, at least, support the suggestion from climate models that increased leakage stimulated convective activity in the North Atlantic hence helping to bring the AMOC out of weak states. The fine-scale variability of our 80 kyr long records suggests that Agulhas leakage carries its own dynamical momentum, which is not driven solely by interhemispheric forcing from the north nor from temperature anomalies associated solely with Antarctic temperature. Comparison with orbital time series and a leakage profile from the penultimate climatic cycle indicates that episodic salt leakage increases may be connected at least in part with obliquity pacing of Southern Hemisphere insolation.

Acknowledgments

Upon publication, data generated as part of this study will be archived in the NCDC Paleoclimatology database: http://www.ncdc.noaa.gov/data-access/paleoclimatology-data. This work was supported by European Commission grant 238512 through the Marie Curie Initial Training Network "GATEWAYS." We thank the International Marine Global Change Studies project and the Institut Polaire Francais Paul Emile Victor, France, for providing core MD02-2594 that was used in this study.

References

Anand, P., H. Elderfield, and M. H. Conte (2003), Calibration of Mg/Ca thermometry in planktonic foraminifera from a sediment trap time series, *Paleoceanography*, *18*(2), 1050, doi:10.1029/2002PA000846.

Arz, H. W., F. Lamy, A. Ganopolski, N. Nowaczyk, and J. Pätzold (2007), Dominant Northern Hemisphere climate control over millennial-scale glacial sea-level variability, *Quat. Sci. Rev.*, *26*(3–4), 312–321, doi:10.1016/j.quascirev.2006.07.016.

Barker, S. (2003), A study of cleaning procedures used for foraminiferal Mg/Ca paleothermometry, *Geochem. Geophys. Geosyst.*, *4*(9), 8407, doi:10.1029/2003GC000559.

Barker, S., P. Diz, M. J. Vautravers, J. Pike, G. Knorr, I. R. Hall, and W. S. Broecker (2009), Interhemispheric Atlantic seesaw response during the last deglaciation, *Nature*, *457*(7233), 1097–1102, doi:10.1038/nature07770.

Bé, A. W. H., and W. H. Hutson (1977), Ecology of planktonic foraminifera and biogeographic patterns of life and fossil assemblages in the Indian Ocean, *Micropaleontology*, *23*(4), 369–414, doi:10.2307/1485406.

Beal, L. M., W. P. M. Ruijter, A. Biastoch, R. Zahn, and SCOR/WCRP/IAPSO Working Group 136 (2011), On the role of the Agulhas system in ocean circulation and climate, *Nature*, *472*(7344), 429–436, doi:10.1038/nature09983.

Bemis, B. E., H. J. Spero, J. Bijma, and D. W. Lea (1998), Reevaluation of the oxygen isotopic composition of planktonic foraminifera: Experimental results and revised paleotemperature equations, *Paleoceanography*, *13*(2), 150–160, doi:10.1029/98PA00070.

Biastoch, A., C. W. Böning, and J. R. E. Lutjeharms (2008a), Agulhas leakage dynamics affects decadal variability in Atlantic overturning circulation, *Nature*, *456*(7221), 489–492, doi:10.1038/nature07426.

Biastoch, A., J. R. E. Lutjeharms, C. W. Böning, and M. Scheinert (2008b), Mesoscale perturbations control inter-ocean exchange south of Africa, *Geophys. Res. Lett.*, *35*, L20602, doi:10.1029/2008GL035132.

Biastoch, A., C. W. Böning, F. U. Schwarzkopf, and J. R. E. Lutjeharms (2009), Increase in Agulhas leakage due to poleward shift of Southern Hemisphere westerlies, *Nature*, *462*, 495–499, doi:10.1038/nature08519.

Boebel, O., J. R. E. Lutjeharms, C. Schmid, W. Zenk, T. Rossby, and C. N. Barron (2003), The Cape Cauldron: A regime of turbulent inter-ocean exchange, *Deep Sea Res., Part II*, *50*, 57–86, doi:10.1016/S0967-0645(02)00379-X.

Boyle, E. A. (1983), Manganese carbonate overgrowths on foraminifera tests, *Geochim. Cosmochim. Acta*, *47*, 1815–1819, doi:10.1016/0016-7037(83)90029-7.

Boyle, E. A., and L. D. Keigwin (1985), Comparison of Atlantic and Pacific paleochemical records for the last 215,000 years: Changes in deep ocean circulation and chemical inventories, *EPSL*, *76*(1–2), 135–150, doi:10.1016/0012-821X(85)90154-2.

Boyle, E. A., and L. D. Keigwin (1987), North Atlantic thermohaline circulation during the past 20,000 years linked to high-latitude surface temperature, *Nature*, *330*, 35–40, doi:10.1038/330035a0.

Broecker, W. S., and G. H. Denton (1989), The role of ocean-atmosphere reorganizations in glacial cycles, *Geochim. Cosmochim. Acta*, *53*(10), 2465–2501, doi:10.1016/0016-7037(89)90123-3.

Caley, T., et al. (2011), High-latitude obliquity as a dominant forcing in the Agulhas current system, *Clim. Past*, *7*(4), 1285–1296, doi:10.5194/cp-7-1285-2011.

Caley, T., J. Giraudeau, B. Malaizé, L. Rossignol, and C. Pierre (2012), Agulhas leakage as a key process in the modes of Quaternary climate changes, *Proc. Natl. Acad. Sci. U.S.A.*, *109*(18), 6835–6839, doi:10.1073/pnas.1115545109.

Caley, T., F. J. C. Peeters, A. Biastoch, L. Rossignol, E. van Sebille, J. V. Durgadoo, B. Malaizé, J. Giraudeau, K. L. Arthur, and R. Zahn (2014), Quanitative estimate of the paleo-Agulhas leakage, *Geophy. Res. Lett.*, *41*, 1238–1246, doi:10.1002/2014GL059278.

Chiang, J. C. H. (2009), The Tropics in Paleoclimate, *Annu. Rev. Earth Planet. Sci.*, *37*(1), 263–297, doi:10.1146/annurev.earth.031208.100217.

Clark, P. U., N. G. Pisias, T. F. Stocker, and A. J. Weaver (2002), The role of the thermohaline circulation in abrupt climate change, *Nature*, *415*(6874), 863–869, doi:10.1038/415863a.

de Ruitjer, W. P. M., A. Biastoch, S. S. Drijfhout, J. R. E. Lutjeharms, R. P. Matano, T. Pichevin, P. J. van Leeuwen, and W. Weijer (1999), Indian-Atlantic interocean exchange: Dynamics, estimation and impact, *J. Geophys. Res.*, *104*(C9), 20,885–20,910, doi:10.1029/1998JC900099.

Durgadoo, J. V., B. R. Loveday, C. J. C. Reason, P. Penven, and A. Biastoch (2013), Agulhas leakage predominantly responds to the Southern Hemisphere westerlies, *J. Phys. Oceanogr.*, *43*, 2113–2131, doi:10.1175/JPO-D-13-047.1.

EPICA Community Members (2006), One-to-one coupling of glacial climate variability in Greenland and Antarctica, *Nature*, *444*(7116), 195–198, doi:10.1038/nature05301.

Ganachaud, A., and C. Wunsch (2000), Improved estimates of global ocean circulation, heat transport and mixing from hydrographic data, *Nature*, *408*(6811), 453–457, doi:10.1038/35044048.

Giraudeau, J., Y. Balut, I. R. Hall, A. Mazaud, and R. Zahn (2003), SWAF-MD128 Scientific Report, Institut Polaire Français, Plouzané, France.

Grant, K. M., E. J. Rohling, M. Bar-Matthews, A. Ayalon, M. Medina-Elizalde, C. B. Ramsey, C. Satow, and A. P. Roberts (2012), Rapid coupling between ice volume and polar temperature over the past 150,000 years, *Nature*, *491*(7426), 744–747, doi:10.1038/nature11593.

Hemleben, C., M. Spindler, and O. R. Erson (1989), *Modern Planktonic Foraminifera*, Springer, Berlin.

Hemming, S. R. (2004), Heinrich Events: Massive Late Pleistocene detritus layers of the North Atlantic and their global climate imprint, *Rev. Geophys.*, *42*, RG1005, doi:10.1029/2003RG000128.

Hodell, D. A., J. E. T. Channell, J. H. Curtis, O. E. Romero, and U. Röhl (2008), Onset of "Hudson Strait" Heinrich events in the eastern North Atlantic at the end of the middle Pleistocene transition (~640 ka)?, *Paleoceanography*, *23*, PA4218, doi:10.1029/2008PA001591.

Huybers, P., and C. Wunsch (2005), Obliquity pacing of the late Pleistocene glacial terminations, *Nature*, *434*(7032), 491–494, doi:10.1038/nature03349.

Jouzel, J., et al. (2007), Orbital and millennial antarctic climate variability over the past 800,000 years, *Science*, *317*(5839), 793–796, doi:10.1126/science.1141038.

JPL (Ed.) (2014), JPL OurOcean Portal, California Institute of Technology. [Available at http://ourocean.jpl.nasa.gov/SST, Accessed 2014.]

Keigwin, L. D., G. A. Jones, S. J. Lehman, and E. A. Boyle (1991), Deglacial meltwater discharge, North Atlantic deep circulation, and abrupt climate change, *J. Geophys. Res.*, *96*(C9), 16,811–16,826, doi:10.1029/91JC01624.

Knorr, G., and G. Lohmann (2003), Southern Ocean origin for the resumption of Atlantic thermohaline circulation during deglaciation, *Nature*, *424*(6948), 532–536, doi:10.1038/nature01855.

Kuhlbrodt, T., A. Griesel, M. Montoya, A. Levermann, M. Hofmann, and S. Rahmstorf (2007), On the driving processes of the Atlantic meridional overturning circulation, *Rev. Geophys.*, *45*, RG2001, doi:10.1029/2004RG000166.

Laskar, J., P. Robutel, F. Joutel, M. Gastineau, A. C. M. Correia, and B. Levrard (2004), A long-term numerical solution for the insolation quantities of the Earth, *Astron. Astrophys.*, *428*(1), 261–285, doi:10.1051/0004-6361:20041335.

Lee, S.-Y., J. C. H. Chiang, K. Matsumoto, and K. S. Tokos (2011), Southern Ocean wind response to North Atlantic cooling and the rise in atmospheric CO_2: Modeling perspective and paleoceanographic implications, *Paleoceanography*, *26*, PA1214, doi:10.1029/2010PA002004.

LeGrande, A. N., and G. A. Schmidt (2006), Global gridded data set of the oxygen isotopic composition in seawater, *Geophys. Res. Lett.*, *33*, L12604, doi:10.1029/2006GL026011.

Lippold, J., J. Grützner, D. Winter, Y. Lahaye, A. Mangini, and M. Christl (2009), Does sedimentary ^{231} Pa/^{230}Th from the Bermuda Rise monitor past Atlantic meridional overturning circulation?, *Geophys. Res. Lett.*, *36*, L12601, doi:10.1029/2009GL038068.

Lisiecki, L. E. (2010), Links between eccentricity forcing and the 100,000-year glacial cycle, *Nat. Geosci.*, *3*(5), 349–352, doi:10.1038/ngeo828.

Lisiecki, L. E., and M. E. Raymo (2005), A Pliocene-Pleistocene stack of 57 globally distributed benthic δ^{18}O records, *Paleoceanography*, *20*, PA1003, doi:10.1029/2004PA001071.

Lisiecki, L. E., M. E. Raymo, and W. B. Curry (2008), Atlantic overturning responses to Late Pleistocene climate forcings, *Nature*, *456*(7218), 85–88, doi:10.1038/nature07425.

Locarnini, R. A., et al. (2013), World Ocean Atlas 2013, in *NOAA Atlas NESDIS 73*, vol. 1: Temperature, edited by S. Levitus and A. Mishonov, 40 pp., U.S. Gov. Print. Off., Washington, D. C.

Loveday, B. R., J. V. Durgadoo, C. J. C. Reason, A. Biastoch, and P. Penven (2014), Decoupling of the Agulhas leakage from the Agulhas Current, *J. Phys. Oceanogr.*, *44*, 1776–1797, doi:10.1175/JPO-D-13-093.1.

Lutjeharms, J. (1996), The exchange of water between the South Indian and the South Atlantic, in *The South Atlantic: Present and Past Circulation*, edited by G. Wefer et al., pp. 122–162, Springer, Berlin.

Marino, G., R. Zahn, M. Ziegler, C. Purcell, G. Knorr, I. R. Hall, P. Ziveri, and H. Elderfield (2013), Agulhas salt-leakage oscillations during abrupt climate changes of the Late Pleistocene, *Paleoceanography*, *28*, 599–606, doi:10.1002/palo.20038.

Martínez-Méndez, G., R. Zahn, I. R. Hall, F. J. C. Peeters, L. D. Pena, I. Cacho, and C. Negre (2010), Contrasting multiproxy reconstructions of surface ocean hydrography in the Agulhas Corridor and implications for the Agulhas Leakage during the last 345,000 years, *Paleoceanography*, *25*, PA4227, doi:10.1029/2009PA001879.

Martrat, B., J. O. Grimalt, C. Lopez-Martinez, I. Cacho, F. J. Sierro, J.-A. Flores, R. Zahn, M. Canals, J. H. Curtis, and D. A. Hodell (2004), Abrupt Temperature Changes in the Western Mediterranean over the Past 250,000 Years, *Science*, *306*(5702), 1762–1765, doi:10.1126/science.1101706.

Martrat, B., J. O. Grimalt, N. J. Shackleton, L. de Abreu, M. A. Hutterli, and T. F. Stocker (2007), Four Climate Cycles of Recurring Deep and Surface Water Destabilizations on the Iberian Margin, *Science*, *317*(5837), 502–507, doi:10.1126/science.1139994.

Mashiotta, T., D. W. Lea, and H. J. Spero (1999), Glacial-interglacial changes in Subantarctic sea surface temperature and δ^{18}O-water using foraminiferal Mg, *EPSL*, *170*(4), 417–432, doi:10.1016/S0012-821X(99)00116-8.

McManus, J. F., D. W. Oppo, and J. L. Cullen (1999), A 0.5-million-year record of millennial-scale climate variability in the North Atlantic, *Science*, *283*(5404), 971, doi:10.1126/science.283.5404.971.

McManus, J. F., R. Francois, J. M. Gherardi, L. D. Keigwin, and S. Brown-Leger (2004), Collapse and rapid resumption of Atlantic meridional circulation linked to deglacial climate changes, *Nature*, *428*(6985), 834–837, doi:10.1038/nature02494.

N. G. R. I. P. Members (2004), High-resolution record of Northern Hemisphere climate extending into the last interglacial period, *Nature*, *431*(7005), 147–151, doi:10.1038/nature02805.

Naik, D. K., R. Saraswat, N. Khare, A. C. Pandey, and R. Nigam (2013), Migrating subtropical front and Agulhas Return Current affect the southwestern Indian Ocean during the late Quaternary, *Clim. Past Discuss.*, *9*(5), 5521–5551, doi:10.5194/cpd-9-5521-2013.

Pahnke, K., and R. Zahn (2005), Southern Hemisphere Water Mass Conversion Linked with North Atlantic Climate Variability, *Science*, *307*(5716), 1741–1746, doi:10.1126/science.1102163.

Pahnke, K., R. Zahn, H. Elderfield, and M. Schulz (2003), 340,000-Year Centennial-Scale Marine Record of Southern Hemisphere Climatic Oscillation, *Science*, *301*(5635), 948–952, doi:10.1126/science.1084451.

Parrenin, F., V. Masson-Delmotte, P. Köhler, D. Raynaud, D. Paillard, J. Schwander, C. Barbante, A. Landais, A. Wegner, and J. Jouzel (2013), Synchronous Change of Atmospheric CO_2 and Antarctic Temperature During the Last Deglacial Warming, *Science*, *339*(6123), 1060–1063, doi:10.1126/science.1226368.

Peeters, F. J. C., R. Acheson, G.-J. A. Brummer, W. P. M. De Ruijter, R. R. Schneider, G. M. Ganssen, E. Ufkes, and D. Kroon (2004), Vigorous exchange between the Indian and Atlantic oceans at the end of the past five glacial periods, *Nature*, *430*(7000), 661–665, doi:10.1038/nature02785.

Pena, L. D., E. Calvo, I. Cacho, S. M. Eggins, and C. Pelejero (2005), Identification and removal of Mn-Mg-rich contaminant phases on foraminiferal tests: Implications for Mg/Ca past temperature reconstructions, *Geochem. Geophys. Geosyst.*, *6*, Q09P02, doi:10.1029/2005GC000930.

Rau, A. J., J. Rogers, J. Lutjeharms, J. Giraudeau, J. A. Lee-Thorp, M.-T. Chen, and C. Waelbroeck (2002), A 450-kyr record of hydrological conditions on the western Agulhas Bank Slope, south of Africa, *Mar. Geol.*, *180*(1), 183–201, doi:10.1016/s0025-3227(01)00213-4.

Rau, A., J. Rogers, and M.-T. Chen (2006), Late Quaternary palaeoceanographic record in giant piston cores off South Africa, possibly including evidence of neotectonism, *Quat. Int.*, *148*(1), 65–77, doi:10.1016/j.quaint.2005.11.007.

Reimer, P. J., et al. (2013), IntCal13 and Marine13 radiocarbon age calibration curves 0-50,000 years cal BP, *Radiocarbon*, *55*(4), 1869–1887, doi:10.2458/azu_js_rc.55.16947.

Rouault, M., P. Penven, and B. Pohl (2009), Warming in the Agulhas Current system since the 1980's, *Geophys. Res. Lett.*, *36*, L12602, doi:10.1029/2009GL037987.

Rühs, S., J. V. Durgadoo, E. Behrens, and A. Biastoch (2013), Advective timescales and pathways of Agulhas leakage, *Geophys. Res. Lett.*, *40*, 3997–4000, doi:10.1002/grl.50782.

Sautter, L. R., and R. C. Thunell (1989), Seasonal succession of planktonic foraminifera; Results from a four-year time-series sediment trap experiment in the Northeast Pacific, *J. Foraminiferal Res.*, *19*, 253–267, doi:10.2113/gsjfr.19.4.253.

Schrag, D. P., J. F. Adkins, K. McIntyre, J. L. Alexander, D. A. Hodell, C. D. Charles, and J. F. McManus (2002), The oxygen isotopic composition of seawater during the Last Glacial Maximum, *Quat. Sci. Rev.*, *21*(1), 331–342, doi:10.1016/s0277-3791(01)00110-x.

Shackleton, N. J., M. A. Hall, and E. Vincent (2000), Phase relationships between millennial-scale events 64,000-24,000 years ago, *Paleoceanography*, *15*(6), 565–569, doi:10.1029/2000PA000513.

Simon, M. H., K. L. Arthur, I. R. Hall, F. J. C. Peeters, B. R. Loveday, S. Barker, M. Ziegler, and R. Zahn (2013), Millenial-scale Agulhas Current variability and its implications for salt-leakage through the Indian-Atlantic Ocean Gateway, *EPSL*, *383*(C), 101–112, doi:10.1016/j.epsl.2013.09.035.

Singh, A., R. A. Jani, and R. Ramesh (2010), Spatiotemporal variations of the δ^{18}O salinity relation in the northern Indian Ocean, *Deep Sea Res., Part I*, *57*(11), 1422–1431, doi:10.1016/j.dsr.2010.08.002.

Skinner, L. C., S. J. Fallon, C. Waelbroeck, E. Michel, and S. Barker (2010), Ventilation of the Deep Southern Ocean and Deglacial CO_2 Rise, *Science*, *328*(5982), 1147–1151, doi:10.1126/science.1183627.

Stocker, T. F. (1998), The Seesaw Effect, *Science*, *282*(5386), 61–62, doi:10.1126/science.282.5386.61.

Stocker, T. F., and S. J. Johnsen (2003), A minimum thermodynamic model for the bipolar seesaw, *Paleoceanography*, *18*(4), 1087, doi:10.1029/2003PA000920.

Toggweiler, J. R., and D. W. Lea (2010), Temperature differences between the hemispheres and ice age climate variability, *Paleoceanography*, *25*, PA2212, doi:10.1029/2009PA001758.

Veres, D., et al. (2013), The Antarctic ice core chronology (AICC2012): An optimized multi-parameter and multi-site dating approach for the last 120 thousand years, *Clim. Past*, *9*(4), 1733–1748, doi:10.5194/cp-9-1733-2013.

Waelbroeck, C., L. C. Skinner, L. Labeyrie, J.-C. Duplessy, E. Michel, N. Vazquez Riveiros, J. M. Gherardi, and F. Dewilde (2011), The timing of deglacial circulation changes in the Atlantic, *Paleoceanography*, *26*, PA3213, doi:10.1029/2010PA002007.

Weijer, W., W. P. De Ruijter, and H. A. Dijkstra (2001), Stability of the Atlantic overturning circulation: Competition between Bering Strait freshwater flux and Agulhas heat and salt sources, *J. Phys. Oceanogr.*, *31*(8), 2385–2402, doi:10.1175/1520-0485(2001)031<2385:SOTAOC>2.0.CO;2.

Weijer, W., W. P. M. De Ruijter, A. Sterl, and S. S. Drijfhout (2002), Response of the Atlantic overturning circulation to South Atlantic sources of buoyancy, *Global Planet. Change*, *34*, 293–311, doi:10.1016/s0921-8181(02)00121-2.

Wolff, E. W., J. Chappellaz, T. Blunier, S. O. Rasmussen, and A. Svensson (2010), Millennial-scale variability during the last glacial: The ice core record, *Quat. Sci. Rev.*, *29*(21–22), 2828–2838, doi:10.1016/j.quascirev.2009.10.013.

Wunsch, C., and R. Ferrari (2004), Vertical mixing, energy, and the general circulation of the oceans, *Annu. Rev. Fluid Mech.*, *36*(1), 281–314, doi:10.1146/annurev.fluid.36.050802.122121.

Ziegler, M., P. Diz, I. R. Hall, and R. Zahn (2013), Millennial-scale changes in atmospheric CO_2 levels linked to the Southern Ocean carbon isotope gradient and dust flux, *Nat. Geosci.*, *6*(6), 457–461, doi:10.1038/ngeo1782.

Auxiliary Material for

Multi-centennial Agulhas leakage variability and links to North Atlantic climate during the past 80,000 years

Kelsey A. Dyez[1]*, Rainer Zahn[1,2], Ian R. Hall[3]

[1]*Institut de Ciència i Tecnologia Ambientals (ICTA), Universitat Autònoma de Barcelona, Bellaterra, 08193, Spain*
**Currently at Lamont-Doherty Earth Observatory, Columbia University, Palisades, NY, 10964, USA*

[2]*Institució Catalana de Recerca i Estudis Avançats (ICREA), Departament de Fisica, Universitat Autònoma de Barcelona, Bellaterra, 08193, Spain*

[3]*School of Earth and Ocean Sciences, Cardiff University, Cardiff, CF10 3AT, UK*

Paleoceanography

Introduction

The Auxiliary Material consists of six supplementary figures. Supplementary Figures (1-6) are referenced in the main body of the manuscript.

Supplementary Figure S1. Agulhas Bank (ABS, MD02-2594, *G. ruber*) and Chatham Rise (MD97-2120, *G. bulloides*) [*Pahnke et al*., 2003; *Pahnke and Zahn*, 2005] SST (a) and planktic $\delta^{18}O$ (b). Green markers are MD97-2120 radiocarbon ages and black markers are MD97-2120_{SST} tie points to Vostock deuterium record. Chatham Rise record is from the south Pacific and 5º farther south than MD02-2594.

Supplementary Figure S2. The MD02-2594 SST record on the timescale of *Martínez-Méndez et al*. [2010] (red) compared to the same record as transferred to the EDC3 timescale (blue).

Supplementary Figure S3. Testing MD02-2594 on the GICC05 timescale. (a) MD02-2594 *G. bulloides* $\delta^{18}O$ on the time scale published by *Martínez-Méndez et al*. [2010] (red) compared with MD02-2594 *G. bulloides* $\delta^{18}O$ on the GICC05 timescale (blue). (b) Age difference (Δ age, black line) along MD02-2594 between the timescales of GICC05 and MM2010 used in (a). Black squares with error bars are ^{14}C age markers along MD02-2594, black squares without error bars are tie points with the EDML time scale [*Martínez-Méndez et al*., 2010]. Blue line is NGRIP maximum counting error for GICC05 from 0-60 kya.

Supplementary Figure S4. Comparison of $\delta^{18}O$ from *G. ruber* (MD02-2594, smoothed to 1000-year windows) and modeled $\delta^{18}O_{sw}$ derived from sea level [*Arz et al*., 2007; *Grant et al*., 2012]. Similar inflection points (marked by arrows) support the age model for core MD02-2594 based on updated calibrations [*Reimer et al*., 2013] for empirical radiocarbon dating.

Supplementary Figure S5. Removal of glacial-interglacial and decadal variability from EDC

δD temperature is achieved by (a) first smoothing the EDC temperature record (gray) to 1000-year windows (blue) and 7500-year windows (orange) [data from *Jouzel et al.*, 2007]. To smooth the record, it was resampled at a high, even spacing (every 10 years) and then averaged within the respective time windows. (b) The difference between the two curves (black curve, Residual T) is the resulting millennial-scale record without decadal or glacial-interglacial variability. As an exercise, we performed the same analysis of EDC δD using the AICC 2012 age model (gray line) [*Veres et al.*, 2013]. (c) Original MD02-2594 SST (red) and the resulting adjusted SST when the millennial-scale contribution from Antarctica is resampled at the sampling resolution of MD02-2594 and subtracted (dark red). The adjusted timeseries using the gray curve from the alternative ice core AICC 2012 age model above (pink). (d) Original $\Delta\delta^{18}O_{sw}$ (green) compared to $\Delta\delta^{18}O_{sw}$ calculated from the residual SST on the EDC ice core age model (dark green) and alternative AICC 2012 age model (blue).

Supplementary Figure S6. Comparison of $\delta^{18}O_{sw}$ changes upstream in the Agulhas Current (CD154 17-17K, orange) [*Simon et al.*, 2013] with Agulhas Bank $\delta^{18}O_{sw}$ (MD02-2594, green).

References:

Arz, H. W., F. Lamy, A. Ganopolski, N. Nowaczyk, and J. Pätzold (2007), Dominant Northern Hemisphere climate control over millennial-scale glacial sea-level variability, *Quaternary Science Reviews*, *26*(3-4), 312–321, doi:10.1016/j.quascirev.2006.07.016.

Grant, K. M., E. J. Rohling, M. Bar-Matthews, A. Ayalon, M. Medina-Elizalde, C. B. Ramsey, C. Satow, and A. P. Roberts (2012), Rapid coupling between ice volume and polar temperature over the past 150,000 years, *Nature*, *491*(7426), 744–747, doi:10.1038/nature11593.

Jouzel, J. et al. (2007), Orbital and Millennial Antarctic Climate Variability over the Past 800,000 Years, *Science*, *317*(5839), 793–796, doi:10.1126/science.1141038.

Martínez-Méndez, G., R. Zahn, I. R. Hall, F. J. C. Peeters, L. D. Pena, I. Cacho, and C. Negre (2010), Contrasting multiproxy reconstructions of surface ocean hydrography in the Agulhas Corridor and implications for the Agulhas Leakage during the last 345,000 years, *Paleoceanography*, *25*(4), PA4227, doi:10.1029/2009PA001879.

Pahnke, K., and R. Zahn (2005), Southern Hemisphere Water Mass Conversion Linked with North Atlantic Climate Variability, *Science*, *307*(5716), 1741–1746, doi:10.1126/science.1102163.

Pahnke, K., R. Zahn, H. Elderfield, and M. Schulz (2003), 340,000-Year Centennial-Scale Marine Record of Southern Hemisphere Climatic Oscillation, *Science*, *301*(5635), 948–952, doi:10.1126/science.1084451.

Reimer, P. J. et al. (2013), IntCal13 and Marine13 radiocarbon age calibration curves 0-50,000

years cal BP, *Radiocarbon*, *55*(4), 1869–1887, doi:10.2458/azu_js_rc.55.16947.

Simon, M. H., K. L. Arthur, I. R. Hall, F. J. C. Peeters, B. R. Loveday, S. Barker, M. Ziegler, and R. Zahn (2013), Millenial-scale Agulhas Current variability and its implications for salt-leakage through the Indian-Atlantic Ocean Gateway, *EPSL*, *383*(C), 101–112, doi:10.1016/j.epsl.2013.09.035.

Veres, D. et al. (2013), The Antarctic ice core chronology (AICC2012): an optimized multi-parameter and multi-site dating approach for the last 120 thousand years, *Climate of the Past*, *9*(4), 1733–1748, doi:10.5194/cp-9-1733-2013.

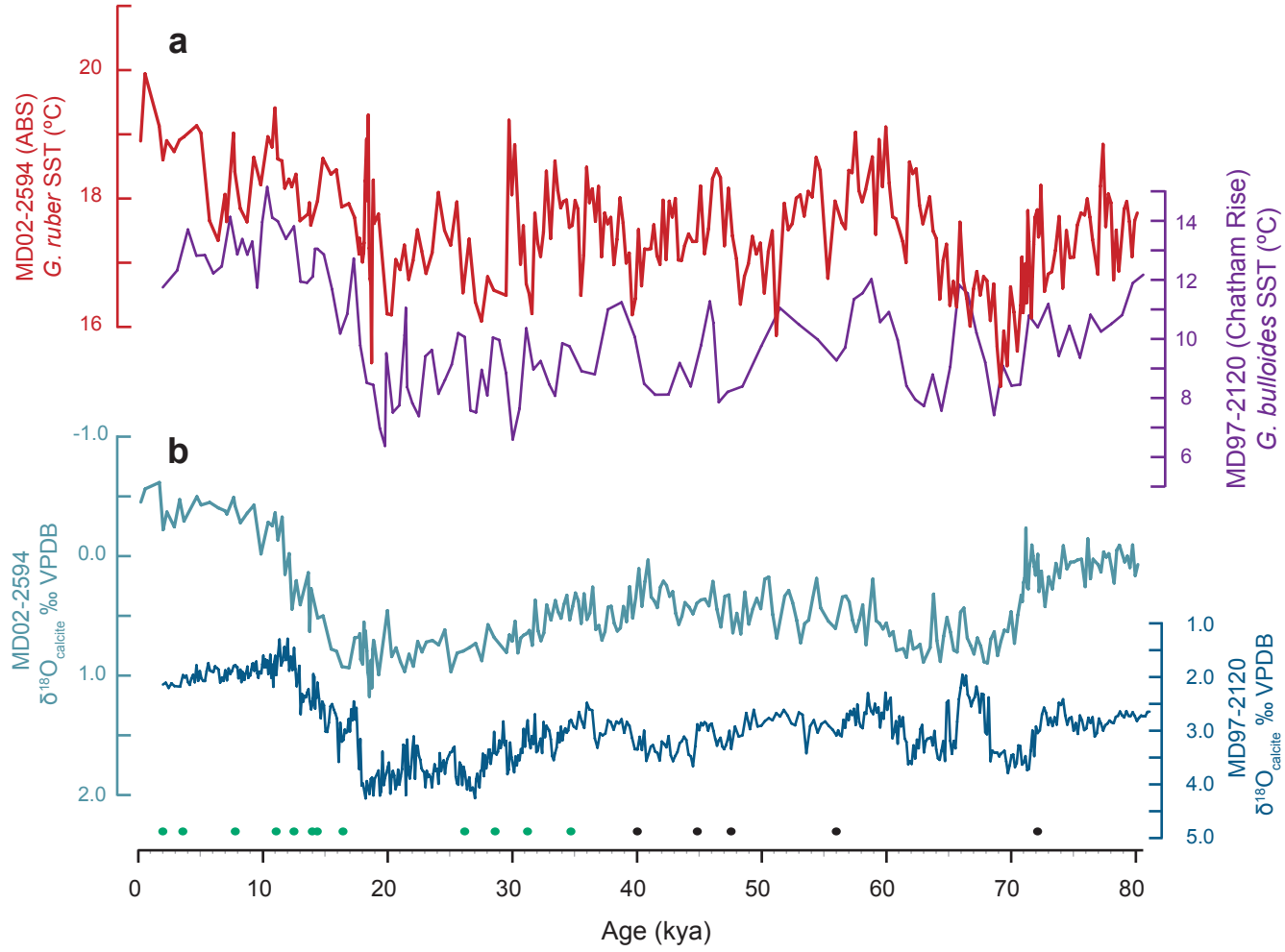
a
b
MD02-2594 (ABS)
G. ruber SST (°C)
MD97-2120 (Chatham Rise)
G. bulloides SST (°C)
MD02-2594
δ18Ocalcite ‰ VPDB
MD97-2120
δ18Ocalcite ‰ VPDB
Age (kya)

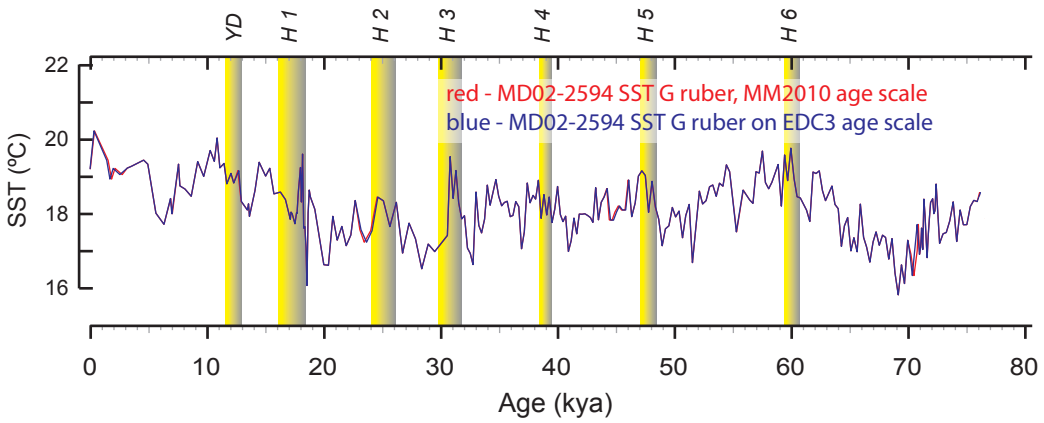
YD
H 1
H 2
H 3
H 4
H 5
H 6
red - MD02-2594 SST G ruber, MM2010 age scale
blue - MD02-2594 SST G ruber on EDC3 age scale
SST (°C)
22
20
18
16
0
10
20
30
40
50
60
70
80
Age (kya)

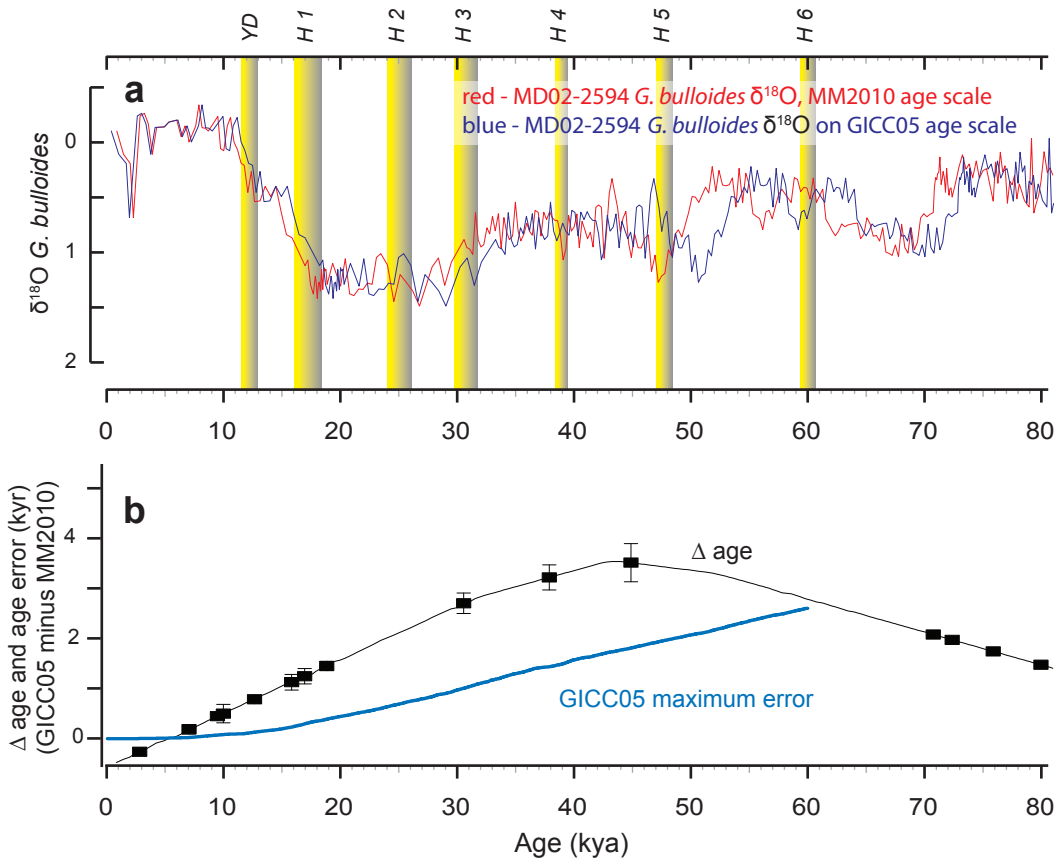
YD
H 1
H 2
H 3
H 4
H 5
H 6
a
red - MD02-2594 G. bulloides δ18O, MM2010 age scale
blue - MD02-2594 G. bulloides δ18O on GICC05 age scale
δ18O G. bulloides
0
1
2
0
10
20
30
40
50
60
70
80
b
Δ age and age error (kyr)
(GICC05 minus MM2010)
Δ age
GICC05 maximum error
0
2
4
0
10
20
30
40
50
60
70
80
Age (kya)

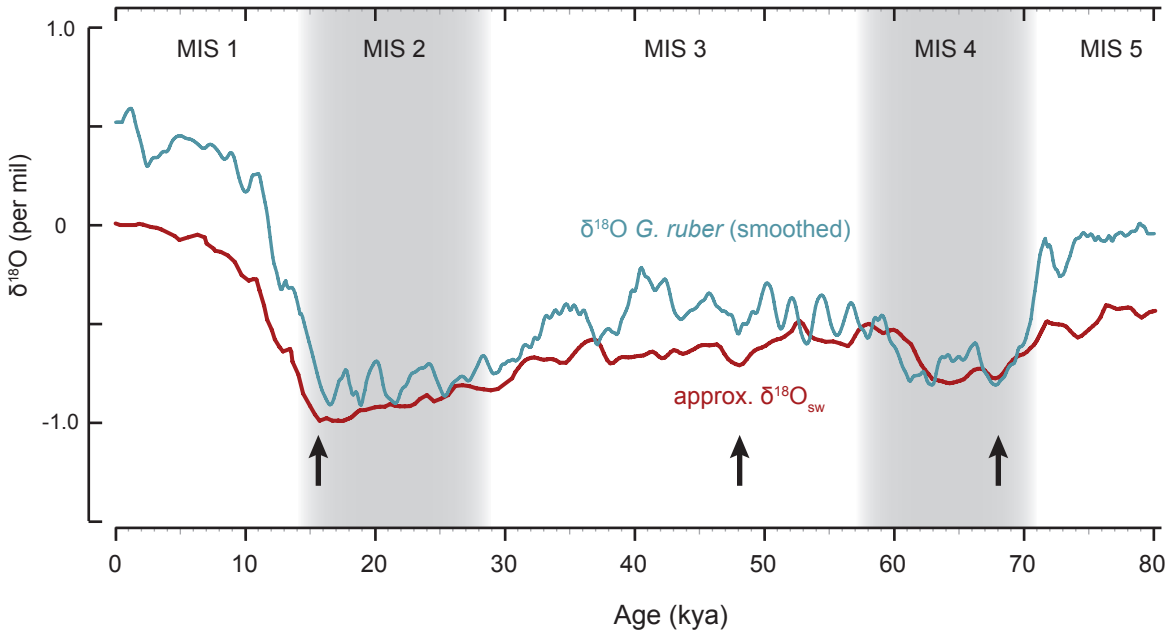
MIS 1
MIS 2
MIS 3
MIS 4
MIS 5
1.0
0
-1.0
δ18O (per mil)
δ18O G. ruber (smoothed)
approx. δ18Osw
0
10
20
30
40
50
60
70
80
Age (kya)

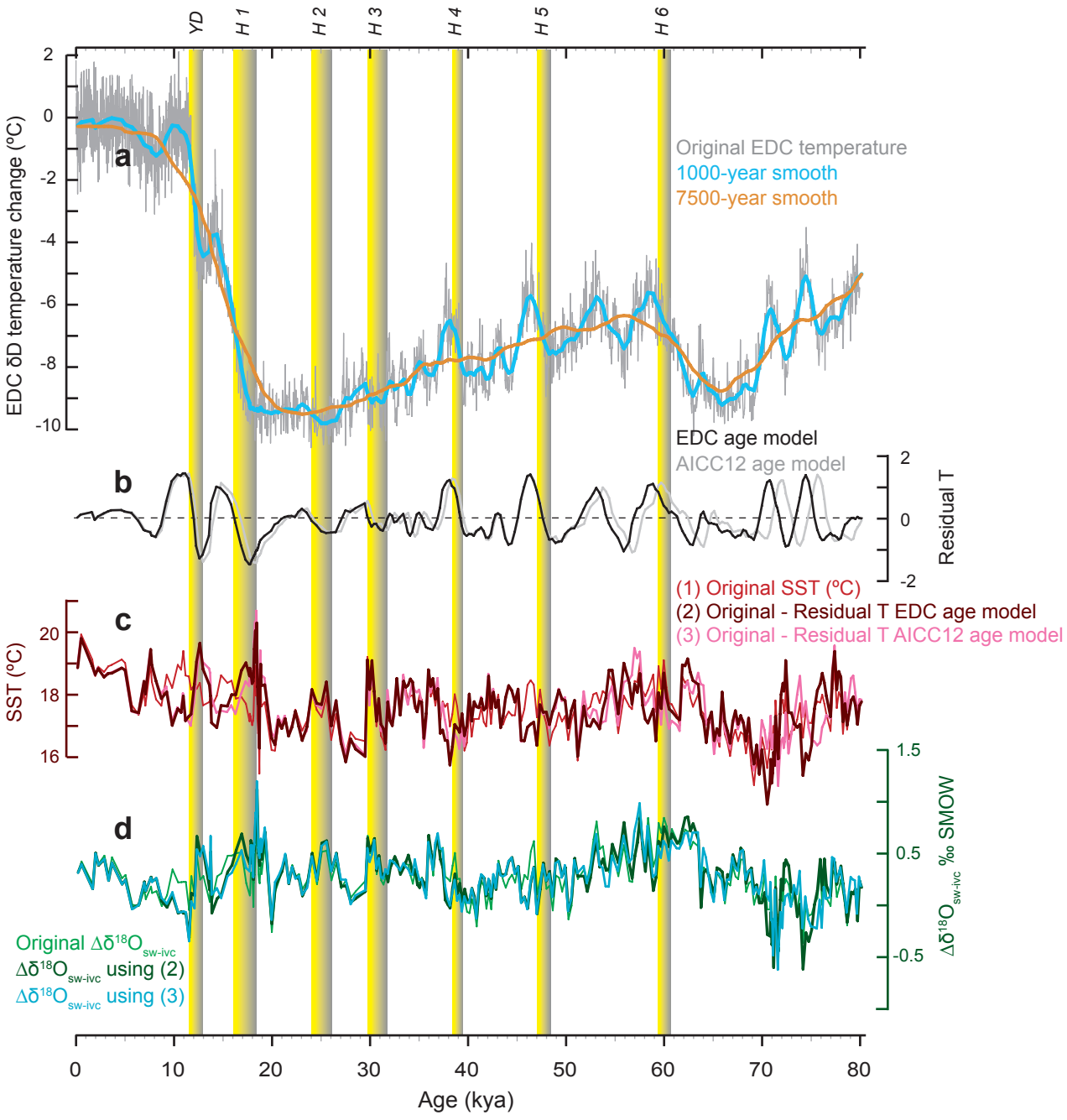
YD
H 1
H 2
H 3
H 4
H 5
H 6
a
EDC δD temperature change (°C)
Original EDC temperature
1000-year smooth
7500-year smooth
b
EDC age model
AICC12 age model
Residual T
c
SST (°C)
(1) Original SST (°C)
(2) Original - Residual T EDC age model
(3) Original - Residual T AICC12 age model
d
Original Δδ18Osw-ivc
Δδ18Osw-ivc using (2)
Δδ18Osw-ivc using (3)
Δδ18Osw-ivc ‰ SMOW
Age (kya)

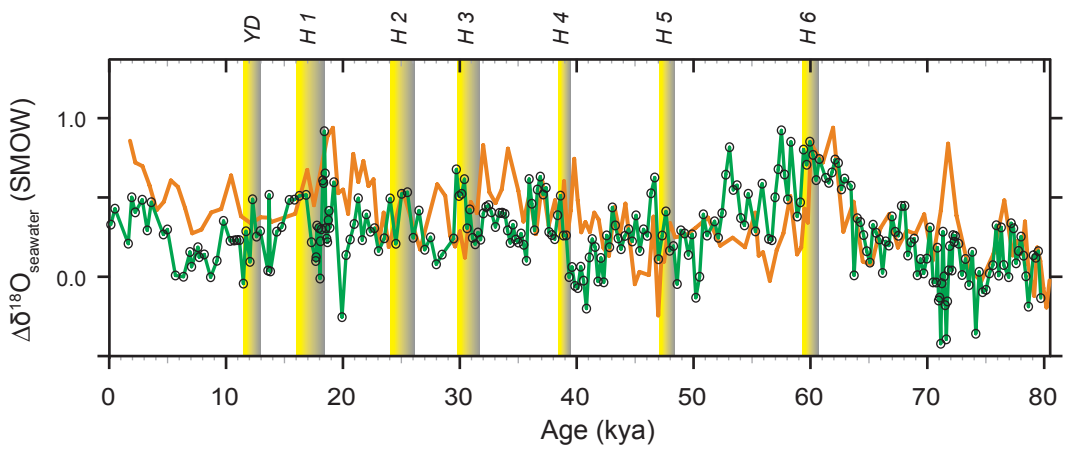
YD
H 1
H 2
H 3
H 4
H 5
H 6
1.0
0.0
$\Delta\delta^{18}O_{seawater}$ (SMOW)
0
10
20
30
40
50
60
70
80
Age (kya)